Since January 2020 Elsevier has created a COVID-19 resource centre with free information in English and Mandarin on the novel coronavirus COVID-19. The COVID-19 resource centre is hosted on Elsevier Connect, the company's public news and information website.

Toxicology and Applied Pharmacology 450 (2022) 116132

Contents lists available at ScienceDirect

Toxicology and Applied Pharmacology

journal homepage: www.elsevier.com/locate/taap

The myosin II inhibitor, blebbistatin, ameliorates pulmonary endothelial barrier dysfunction in acute lung injury induced by LPS via NMMHC IIA/Wnt5a/β-catenin pathway

Jiazhi Zhang [1], Ziqian Pan [1], Jianhao Zhou, Ling Zhang, Jiahui Tang, Shuaishuai Gong, Fang Li, Boyang Yu, Yuanyuan Zhang [*], Junping Kou [*]

State Key Laboratory of Natural Medicines, Jiangsu Key Laboratory of TCM Evaluation and Translational Research, Department of Pharmacology of Chinese Materia Medica, School of Traditional Chinese Pharmacy, China Pharmaceutical University, Nanjing 211198, China

ARTICLE INFO

Editor: Lawrence Lash

Keywords:
Blebbistatin
Acute lung injury
Pulmonary endothelial barrier
Non-muscle myosin IIA
Signaling pathway

ABSTRACT

Acute lung injury (ALI) or its most advanced form, acute respiratory distress syndrome (ARDS), is a severe inflammatory pulmonary process triggered by varieties of pathophysiological factors, among which endothelial barrier disruption plays a critical role in the progression of ALI/ARDS. As an inhibitor of myosin II, blebbistatin inhibits endothelial barrier damage. This study aimed to investigate the effect of blebbistatin on lung endothelial barrier dysfunction in LPS induced acute lung injury and its potential mechanism. Mice were challenged with LPS (5 mg/kg) by intratracheal instillation for 6 h to disrupt the pulmonary endothelial barrier in the model group. Blebbistatin (5 mg/kg, ip) was administrated 1 h before LPS challenge. The results showed that blebbistatin could significantly attenuate LPS-induced lung injury and pulmonary endothelial barrier dysfunction. And we observed that blebbistatin inhibited the activation of NMMHC IIA/Wnt5a/β-catenin pathway in pulmonary endothelium after LPS treatment. In murine lung vascular endothelial cells (MLECs) and human umbilical vein endothelial cells (HUVECs), we further confirmed that Blebbistatin (1 μmol/L) markedly ameliorated endothelial barrier dysfunction in MLECs and HUVECs by modulating NMMHC IIA/Wnt5a/β-catenin pathway. Our data demonstrated that blebbistatin could inhibit the development of pulmonary endothelial barrier dysfunction and ALI via NMMHC IIA/Wnt5a/β-catenin signaling pathway.

1. Introduction

Acute lung injury (ALI) is a severe inflammatory disease of the lungs with high morbidity and mortality, characterized by respiratory distress, progressive hypoxemia, and pulmonary edema. At present, there are no effective therapeutic drugs and preventive strategies for ARDS in clinical practice. Although mechanical ventilation and restrictive fluid management have been widely used in lung protection with the deepening of the study on the pathological mechanism of ARDS, the mortality rate of ARDS is still up to 50% (Villar et al., 2016). The membrane barrier formed by endothelial cells, epithelial cells, and their fused basal layer in lung tissue maintains the rapid and effective exchange of gaseous substances between alveoli and blood vessels. Under physiological conditions, the barrier protects against the invasion of harmful substances such as particulate matter and microorganisms inhaled from the outside, playing a significant role in the body (Müller Redetzky et al., 2014). Under pathological conditions, the dysfunction of the pulmonary endothelial barrier can lead to increased vascular permeability, pulmonary edema, and the accumulation of a large number of inflammatory cells, thus affecting the exchange of gas and blood, resulting in hypoxemia and respiratory failure, which eventually induces acute respiratory distress syndrome (ARDS) (Thompson et al., 2017). Therefore, pulmonary vascular endothelial barrier dysfunction is the most critical pathophysiological feature in the early stage of ALI/ARDS (Millar et al., 2016; Bhattacharya and Matthay, 2013). It is an essential strategy for the clinical prevention and treatment of ALI/ARDS that maintains the integrity of pulmonary vascular endothelial barrier.

It is well known that adherens junction (AJs) is a significant component of the pulmonary endothelial junction, and VE-cadherin, as one of the crucial components of AJs, plays a vital role in maintaining

* Corresponding authors.
E-mail addresses: yuanyuanzhang@cpu.edu.cn (Y. Zhang), junpingkou@cpu.edu.cn (J. Kou).
[1] These authors contributed equally to this article.

https://doi.org/10.1016/j.taap.2022.116132
Received 11 March 2022; Received in revised form 10 June 2022; Accepted 13 June 2022
Available online 15 June 2022

the integrity of pulmonary endothelial barrier (Gong et al., 2015; Dong et al., 2018). Meanwhile, β-catenin involves regulating microvascular endothelial cell hyperpermeability, which is positively associated with endothelial VE-cadherin stability (Rho et al., 2017; Tharakan et al., 2012). Therein, the extracellular region of VE-cadherin is clustered between adjacent endothelial cells by homologous binding, and the intracellular part of VE-cadherin is mainly bound to the catenin family. The C-terminal area of VE-cadherin intracellular tail anchors α-catenin by binding to β-catenin, thereby promoting the interaction between VE-cadherin and the cytoskeleton. In the process of endothelial barrier dysfunction caused by stimulating factors, phosphorylation of the binding site of VE-cadherin and β-catenin leads to degradation of VE-cadherin and β-catenin, resulting in reduced expression of adhesive connexins on endothelial cell membranes. For example, in the process of LPS or TNF-α-induced lung endothelial barrier damage, the expression of β-catenin and VE-cadherin in lung tissue is significantly reduced (Liu et al., 2012; Gong et al., 2008; Xiao et al., 2005). These drugs can dramatically protect the pulmonary vascular endothelial barrier function and improve the survival rate of ARDS mice by inhibiting the expression of β-catenin and VE-cadherin (Yu et al., 2016; Chen et al., 2018). The Wnt/β-catenin signaling pathway is involved in regulating various physiological and biochemical functions. Meanwhile, the relationship between Wnt/β-catenin and ALI has been studied early (Hii et al., 2015). Among them, studies have shown that the expression of Wnt5a is elevated in the ALI model, and inhibiting Wnt5a attenuates the progress of ALI (Villar et al., 2014). In summary, the Wnt5a/β-catenin signaling pathway in endothelial cells is closely related to the pulmonary endothelial barrier.

Non-muscle myosin heavy chain IIA (NMMHC IIA), the primary subtype of type-II non-muscle myosin (NMM II), is a crucial protein regulating body growth and barrier function (Wang et al., 2020a, 2020b; Zhai et al., 2017). Previous studies showed that NMM II knockdown improves survival and therapeutic effects of implanted bone marrow-derived mesenchymal stem cells in lipopolysaccharide-induced acute lung injury (Wu et al., 2021). Meanwhile, konckout non-muscle myosin light kinase (nmMLCK),a factor closely related to NMMHC IIA, can improve lung endothelial cell inflammation and lung PMN infiltration stimulated by a variety of factors (Sun et al., 2021; Fazal et al., 2013). Furthermore, in NMMHC IIA knockout mice, endodermal abnormalities were observed during embryonic development, during which E-cadherin and β-catenin levels were significantly decreased, and the embryos died on day 7.5 (Conti et al., 2004). At the same time, it has been reported that the loss of NMMHC IIA in epithelial cells can spontaneously cause an increase in intestinal epithelial barrier permeability, which is mainly manifested as increased infiltration of lymphocytes, increased release of inflammatory factors, and decreased content of β-catenin, p120-catenin, and occludin protein-7. And in the experimental colitis model, intestinal barrier and mucosal damage were aggravated in the epithelial NMMHC IIA deficient mice compared with the control mice (Naydenov et al., 2016). These findings suggest that NMMHC IIA regulates the expression of β-catenin, thereby affecting barrier function. Moreover, NMMHC IIA is involved significantly in endothelial barrier regulation, and its overexpression leads to endothelial barrier dysfunction (Gong et al., 2021; Wu et al., 2021). Meanwhile, NMMHC IIA targeted drugs and endothelium-specific allelic knockout of NMMHC IIA can improve the LPS-induced decrease of VE-cadherin expression in lung tissues and play a role in protecting the lung endothelial barrier function.

Previous studies have shown that blebbistatin (a non-specific inhibitor of NMMHC IIA) ameliorates endothelial barrier-injury induced by OGD/R in vitro and inhibits cerebral I/R injury-induced BBB disruption in vivo. However, whether and how blebbistatin regulates pulmonary endothelial barrier disruption to inhibit LPS-induced ALI.

In the present study, we observed the effect of blebbistatin on LPS-induced pulmonary endothelial barrier dysfunction through modulating NMMHC IIA/Wnt5a/β-catenin signaling pathway in vivo and in vitro. These findings suggest that blebbistatin may have potential clinical application in the prevention and treatment of ALI and explain the underlying mechanism by which blebbistatin protects endothelial barrier function.

2. Materials and methods

2.1. Reagents and antibodies

Lipopolysaccharide LPS L2880 was obtained from Sigma-Aldrich St. Louis, MO, USA. A myeloperoxidase (MPO) assay kit was purchased from Nanjing Jiancheng Bioengineering Institute (Nanjing, China). Anti-CD31 (AF3628) was purchased from R&D Systems (Minneapolis, MN, USA). Anti-MYH9 (11128–1-AP) and anti-IgG (B900610) were purchased from Proteintech Group (Chicago, IL, USA). Anti-Wnt5a (sc-365,370), Anti-β-catenin (sc-7963), Anti-TLR4 (sc293072), and Protein A/G PLUS-Agarose (sc-2003) were obtained from Santa Cruz Biotechnology Inc. (Texas, CA, USA). Anti-VE-cadherin (ab33168) was provided by Abcam (Cambridge, MA, USA). Duolink®In Situ PLA® Probe Anti-Rabbit PLUS (DUO92002), Duolink® In Situ PLA® Probe Anti-Mouse MINUS (DUO92004), and Duolink®In Situ Detection Reagents Red (DUO92008) were obtained from Sigma–Aldrich (St. Louis, MO, USA).

The bicinchoninic acid (BCA) protein assay kit and phenylmethanesulfonyl fluoride (PMSF) were procured from Beyotime Biotechnology (Shanghai, China). Alexa Fluor 488- and 594-conjugated secondary antibodies and Dynabeads™ Sheep Anti-Rat IgG (11035) were from Thermo Fisher Scientific (Waltham, MA, USA).

2.2. Animal experiments

C57BL/6 male mice (18–22 g) were provided by the Experimental Animal Center of Yangzhou University (Certificate number was SCXK 2020–0011). After 3 days of adjustable feeding, the mice were randomly divided into four groups ($n = 6$): control group, control +Ble (5 mg/kg), ALI group, and ALI + Ble (5 mg/kg) groups. After inhalation anesthesia with isoflurane, the mice in the ALI group were challenged with LPS (5 mg/kg) by intratracheal instillation for 6 h. At the same time, sterile saline was used in the control group. Blebbistatin was intraperitoneally injected 1 h before LPS treatment. All mice were euthanized after LPS induction, and lung tissues were collected for the subsequent experiments. All experimental animal procedures were carried out according to the National Institutes of Health guidelines, and the Animal Ethics Committee approved the protocols of China Pharmaceutical University.

2.3. Histopathological analysis

Lung tissues fixed in 4% paraformaldehyde were embedded in paraffin, cut into 4-μm sections, and stained with hematoxylin and eosin (H&E). Pathological images were examined using an optical microscope (Nikon, Japan), and pathologists scored the extent of the injury.

2.4. Lung EB-albumin leakage

Mice were intravenously injected with EB-albumin (50 mg/kg) via the tail vein at 4 h after LPS exposure and perfused 2 h later with PBS containing 5 mM EDTA-2Na on the right ventricle to remove the intravascular dye from the lung. Lung tissues were collected, flash-frozen in liquid nitrogen, and homogenized in a ten-fold volume of formamide. The homogenate was incubated at 60 °C for 18 h. After centrifugation at 5000 $\times g$ for 30 min, the absorption of EB in the supernatant was measured at 620 nm, and the EB content was measured with a standard curve.

2.5. BALF cell count

The BALF was centrifuged at 4 °C, 1500 rpm for 10 min, and the

precipitate was resuspended in 500 μL PBS. Cell amounts of total cells were calculated using a blood analyzer (ADVIA 2120, Siemens, Germany).

2.6. Determination of the MPO content

According to the corresponding manufacturer's instructions, the MPO content in the BALF and lung were determined using assay kits.

2.7. Immunofluorescence assays

The frozen sections (10 μm) of lung tissues were fixed with 4% formaldehyde and permeabilized with 0.1% Triton X-100, then blocked with 5% bovine serum albumin (BSA) and probed with the following primary antibodies overnight at 4 °C: CD31 (1:100 dilution, R&D Systems, USA), VE-cadherin (1:100 dilution, Abcam, USA), MYH9 (1:200 dilution, Proteintech, USA), Wnt5a (1:50 dilution, Santa Cruz Biotechnology Inc., USA), β-catenin (1:50 dilution, Santa Cruz Biotechnology Inc., USA). The next day the appropriate fluorescence-conjugated secondary antibodies were used: Alexa Fluor 594-donkey anti-goat IgG (A11058), Alexa Fluor 488-goat anti-mouse IgG (A21202), and Alexa Fluor 488-donkey anti-rabbit IgG (A21206) (1:500 dilution, Thermo Fisher Scientific, USA). Fluorescent images were visualized using confocal laser scanning microscopy (CLSM, LSM700, Zeiss, Germany).

2.8. Cell culture

Human umbilical vein endothelial cells were purchased from the Shanghai Institute of Cell Biology, Chinese Academy of Sciences. HUVECs were grown in RPMI 1640 medium (Invitrogen Life Technologies, Carlsbad, CA, USA) supplemented with 10% heat-inactivated fetal bovine serum (FBS, ScienCell, CA, USA), 100 U/mL penicillin, 100 μg/mL streptomycin, and 2.0 g/L sodium bicarbonate. Cells were maintained at 37 °C with 95% humidity and 5% CO_2.

MLECs isolation and culture MLECs were isolated as described previously(Lim et al., 2003).

In brief, the lung lobes harvested from four mice were carefully dissected out from bronchus and mediastinal connective tissues. After being washed in 25 ml Dulbecco's modified Eagle's medium (DMEM) (Gibco, USA) containing 10% fetal bovine serum FBS Gibco, USA, the organs were minced with sterile stainless steel blades for 10 min and digested in 25 ml of collagenase at 37 °C for 1 h. Then the digested tissue was filtered through a clean 70 μm cell strainer Corning, 352,350 and centrifuged at 1500 rpm for 10 min at 4 °C. The cell pellet was resuspended in 0.1% BSA-PBS and incubated with CD31-coated magnetic beads (Dynabeads™ Sheep Anti-Rat IgG, 11,035, Thermo Fisher Scientific, USA) at room temperature for 15 min with end-over-end rotation. The bead-bound cells were recovered by a magnetic separator and washed with DMEM-10% FBS. Then the recovered cells were suspended and cultured in DMEM supplemented with 20% FBS, 1%MEM Non-Essential Amino Acids, 2.5% HEPES buffer solution (1 M) (Gibco, USA), endothelial cell growth supplement (0.1 mg/ml) (Sigma, USA), 100 U/mL penicillin and 100 U/mL streptomycins (Gibco, USA) at 37 °C in a humidified incubator of 5% CO_2 and 95% air.

Transendothelial Electrical Resistance (TEER) Assays and EB-albumin leakage Assays.

Human umbilical vein endothelial cells were seeded on transwell inserts (0.4 μM pore, 6.5 mm diameter, Millipore, USA) for 7 days. The TEER of the monolayer was also measured daily with a Millicell-ERS voltmeter (Millipore, USA). Resistance values of multiple transwell inserts of an experimental group were calculated sequentially. The mean was expressed in the standard unit (Ω·cm2) after subtracting a blank cell-free filter value. The TEER of the monolayers was recorded when a stable resistance reading was achieved with triplicate measurements taken for each transwell. Blebbistatin (1 μmol/L) was added to the inner and outer chamber for 1 h, and 5 μg/mL LPS was added for 6 h. The inner chamber fluid was changed to 200 μL EB-albumin solution as the tracer, and the outer chamber fluid was changed to 600 μL 4% BSA solution and incubated in an incubator for 1 h. Collect the extracellular fluid, add 200 μL per well to the 96-well plate, measure the absorbance at 620 nm, and calculate the content of EB-albumin leakage according to the EB curve.

2.9. Flow cytometry

The second generation of lung endothelial cells was digested with trypsin solution and repeatedly blown to the cell suspension. After washing with PBS, cells were incubated with FcR blocking agent (Miltenyi, Germany) for 10 min at 4 °C. Then, cells were incubated with VE-cadherin (Miltenyi, Germany) for 30 min on ice, followed by 30 min secondary antibody incubation with PBS washing between the incubation periods. Samples were run on the FACScan flow cytometer(Miltenyi, Germany). Analyses were performed using FlowJo software. Surface antigen levels were expressed as the mean fluorescence intensity of cells.

2.10. Western blot analysis

The total protein extracted from HUVECs or lung tissues was quantified using a BCA protein assay kit (Nanjing Jiancheng Bioengineering Institute, Nanjing, China). Equal amounts of total protein (30 μg) in each group were separated by SDS-PAGE gels and transferred to PVDF membranes. Then the membranes were blocked in 5% BSA for 2 h and incubated overnight at 4 °C with the following primary antibodies: VE-cadherin (1:1000 dilution, Abcam, USA), Wnt5a, and β-catenin (1:500 dilution, Santa Cruz Biotechnology, USA), MYH9 (1:8000 dilution, Proteintech, USA). After washing three times with TBST, the membranes were incubated with HRP anti-conjugated secondary antibodies for 1.5 h at room temperature. The bands were detected using an ECL kit (Vazyme Biotechnology, Nanjing, China) and analyzed with Image Lab™ Software.

2.11. Immunofluorescence co-localization analysis

To evaluate the amount of co-localization between two stains in the images, the plugin JaCoP in Image J (National Institutes of Health, Bethesda, MD, USA) was used in pixel matching co-localization analyses (Bolte and Cordelières, 2006). In brief, two different channels in one image were processed by Image J. Then all correlation-based co-localization were obtained, and information of microscope (CLSM, LSM700; Zeiss) and the emitted wavelength of fluorescence were entered into the JaCoP., After regulating the threshold, the co-localization was evaluated with the manders' co-localization coefficients.

2.12. Co-immunoprecipitation (Co-IP) assay

Cell lysates were incubated with an equal amount of NMMHC IIA antibody or IgG antibody, followed by incubation with an equal amount of Protein A/G PLUS Agarose. Proteins were divided by SDS-PAGE followed by Western blot analysis.

2.13. Proximity ligation assays (PLA)

A PLA kit (DUO92004, DUO92008, and DUO92002; Sigma–Aldrich) was employed to detect interactions between NMMHC IIA and TLR4 in MLECs, according to the manufacturer's protocols(Pierre and Scholich, 2010). Samples were incubated with primary antibodies for TLR4 and NMMHC IIA. Secondary antibodies, conjugated with PLA probes, were added to the reaction for subsequent ligation and rolling circle amplification. Images were observed under a CLSM (LSM700; Zeiss) and processed using ZEN imaging software.

2.14. Statistical analysis

All data were presented as mean ± standard deviations (SDs) and analyzed with GraphPad Prism software (version 8.0). Statistical significance was calculated with a one-way analysis of variance (ANOVA) followed by Dunnett's test. Differences were considered significant at P values <0.05.

3. Results

3.1. Effects of blebbistatin on the LPS-induced pulmonary pathological damage and pulmonary inflammation in mice

To determine the effects of blebbistatin in vivo, the ALI mice model was established by intratracheal instillation of LPS. Mice were intraperitoneally injected with blebbistatin (5 mg/kg) before intratracheal LPS (5 mg/kg) injection, and lung tissues and BALF were collected at 6 h after LPS challenge. The results of H&E showed that after pretreatment with blebbistatin (5 mg/kg), the damage of the lung was significantly less than that in the model group. Calculation of lung injury scores and lung coefficient results indicated that blebbistatin protected against pulmonary lesions (Fig. 1, A and B). Meanwhile, the lung index and the lung W/D ratio results showed that blebbistatin could significantly alleviate pulmonary edema in the model group (Fig. 1, C and D). Above all, these results reflected that blebbistatin could protect against pulmonary pathological damage. Next, we measured the total cell counts and protein in BALF. The results showed that blebbistatin significantly inhibited the number of complete cell counts and protein (Fig. 1, E and F). MPO is present in neutrophils, accounting for about 5% of cell dry weight, reflecting the number of neutrophils (Kitching et al., 2020; Gorudko et al., 2018). Therefore, MPO levels were measured in BALF and lung tissue to measure inflammation levels. The MPO assay results showed that compared with the model group, blebbistatin (5 mg/kg) significantly inhibited the increase of MPO expression in both BALF and lung tissue (Fig. 1, G and H). Collectively, these findings showed that blebbistatin significantly improved pulmonary pathological damage and pulmonary inflammation in ALI initiated due to LPS.

3.2. Effect of blebbistatin on LPS-triggered lung endothelial barrier dysfunction in mice

Impaired pulmonary vascular endothelial barrier function is a typical pathological feature of ALI. To determine the effects of blebbistatin on LPS-induced pulmonary vascular hyperpermeability, mice were

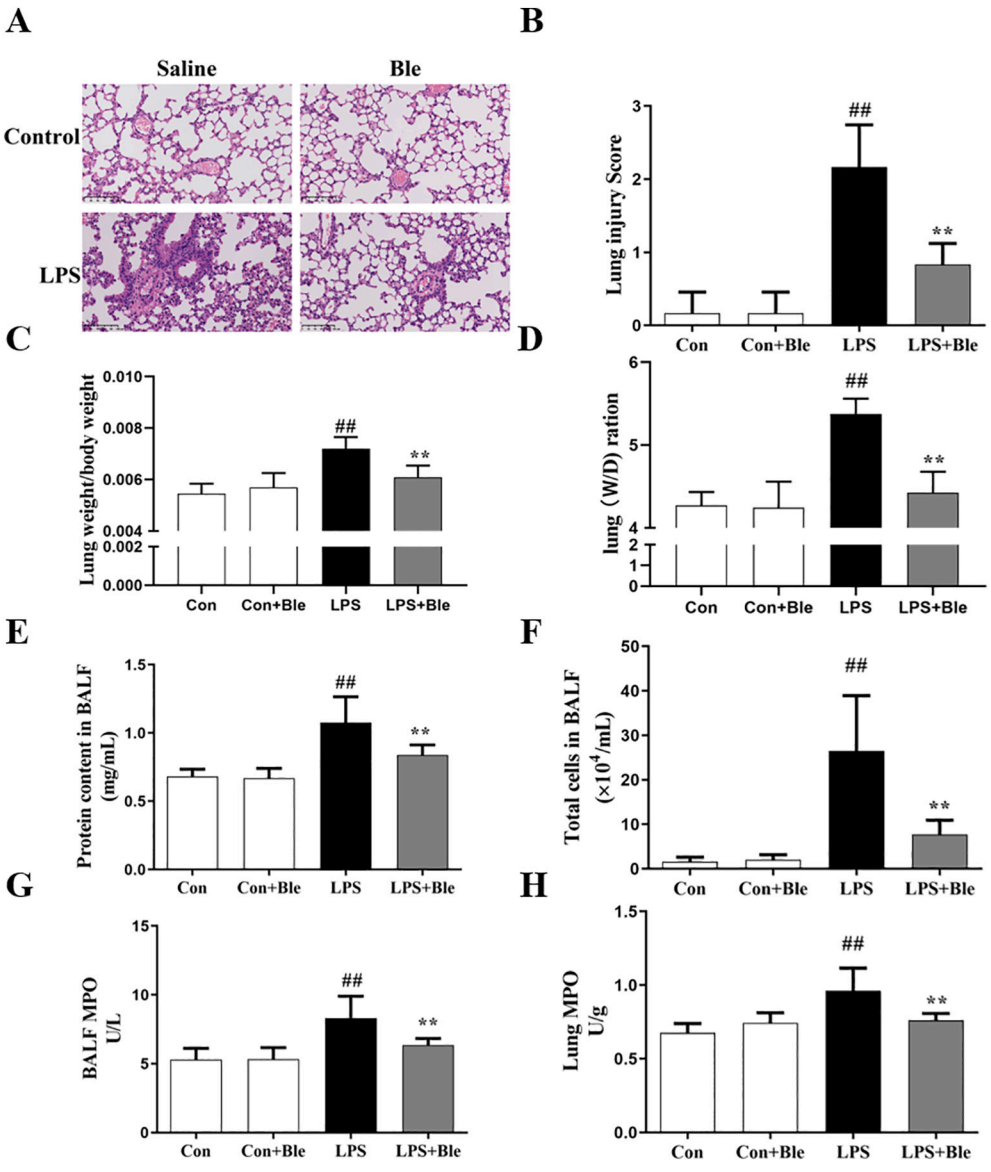

Fig. 1. Blebbistatin mitigated LPS-induced pulmonary pathological damage and pulmonary inflammation in mice. Mice were injected intraperitoneally with blebbistatin (5 mg/kg) for 1 h prior to LPS instillation for 6 h. The lung and BALF was collected. (A) Effects of blebbistatin on LPS-induced lung histopathological changes were determined in mice by H&E staining. (B) The effects of blebbistatin on LPS-induced lung morphology. The lung tissue slices were histopathologically assessed using a semi-quantiative scoring method. Lung injury was graded from 0 (normal) to 4 (severe) in four categories: inflammatory cell infiltration, edema, congestion and interstitial inflammation. The total lung injury score was calculated by adding up the individual scores of each category. The effects of blebbistatin on (C) the lung index and (D) the lung W/D ratio were determined in LPS-induced ALI mice. The effects of blebbistatin on LPS-induced increase of (E) protein and (F) total cell counts were determined in BALF. (G-H) The effects of blebbistatin on LPS-induced increase of MPO activity were determined in BALF and lung tissues. Data are shown as the means ± SD (A-B). $n = 3$. (C–H). $n = 8$. $^{\#\#}P < 0.01$ vs. the control group; $^{**}P < 0.01$ vs. the LPS group. The scale bar is 100 μm.

intravenously injected with Evans blue-albumin (EBA) at 4 h after LPS administration. Then, the dye was extracted from lung tissues and quantified after 2 h. The mice lung gross morphology result showed that after injection of Evans blue dye, the lung of model mice became utterly blue, but the lung of mice treated with blebbistatin (5 mg/kg) remained pale (Fig. 2A). The EB-albumin leakage and immunofluorescence results disclosed that a rapid increase in albumin leakage in the lung tissues of model mice was observed, and this increase was inhibited via blebbistatin treatment (Fig. 2, B and C). VE-cadherin protein is a vital component of the adhesion structure between vascular endothelial cells, and its protein content represents the damage degree of the barrier. Blebbistatin significantly inhibited the reduction of VE-cadherin content in lung tissues induced by LPS at different modeling time points, thus protecting the endothelial barrier from LPS injury (Fig. 3, A-C). These results suggested that blebbistatin protected the lung endothelial barrier in LPS-triggered ALI in mice.

3.3. Effect of blebbistatin on the NMMHC IIA/Wnt5a/β-catenin signaling pathway in LPS-induced pulmonary endothelium

To determine the mechanism by which blebbistatin protected against pulmonary endothelial barrier dysfunction, we observed the expression of the endothelial barrier-related factors NMMHC IIA, Wnt5a, and β-catenin in pulmonary endothelium. Immunofluorescence staining results showed that in CD31-labeled mouse lung endothelial cells, blebbistatin administration significantly inhibited the increase of NMMHC IIA and Wnt5a expression levels in the lung endothelial cells of the model group (Fig. 4 A and B), and blebbistatin administration significantly inhibited the decrease of β-catenin expression level in the lung endothelial cells of the model group (Fig. 4C). These data indicated that blebbistatin abolished LPS-induced activation of the NMMHC IIA/Wnt5a/β-catenin pathway in the pulmonary endothelium.

3.4. Effect of blebbistatin on LPS-induced endothelial barrier dysfunction in MLECs

To further verify the endothelial barrier protective effect of blebbistatin in vitro, MLECs were specifically isolated with purified rat anti-mouse CD31 monoclonal antibody-coated magnetic beads and identified by immunofluorescence. MLECs were pretreated with blebbistatin (1 μmol/L) for 1 h, then stimulated with 5 μg/mL LPS. The TEER results demonstrated that LPS stimulated lung endothelial cells for 1 h to 24 h. The transendothelial resistance decreased continuously. After the administration of blebbistatin, LPS induced TEER decreased significantly, protecting pulmonary vascular endothelial barrier function. Meanwhile, it does not affect transendothelial resistance (Fig. 5A). Meanwhile, blebbistatin significantly inhibited the increase of EBA leakage in LPS-induced MLECs cells (Fig. 5B). The flow cytometry results showed that the content of VE-cadherin in the membrane of lung endothelial cells was significantly decreased 6 h after LPS stimulation, and blebbistatin significantly reversed the LPS-induced decrease of VE-cadherin content in the membrane of lung endothelial cells (Fig. 5, C and D). Collectively, blebbistatin protected against LPS-induced MLECs barrier disruption.

3.5. Effect of blebbistatin on LPS-induced endothelial barrier dysfunction in HUVECs

To further clarify the effect of blebbistatin in inhibiting LPS-induced endothelial barrier dysfunction, HUVECs were used in this section, and LPS exposure models were established. HUVECs were pretreated with blebbistatin (1 μmol/L) 1 h before LPS (5 μg/mL) exposure and the TEER of HUVECs was examined, and the samples of HUVECs were collected at 6 h after LPS challenge. After 6 h of LPS stimulation, blebbistatin (1 μmol/L) significantly elevated the TEER value of HUVECs (Fig. 6A). Meanwhile, blebbistatin significantly inhibited the increase of EBA leakage in LPS-induced HUVECs cells (Fig. 6B). Finally, the western blot results showed that blebbistatin (1 μmol/L) significantly inhibited the decrease of VE-cadherin in HUVECs of the model group (Fig. 6C). These results suggested that blebbistatin could protect LPS-induced endothelial cell barrier dysfunction in HUVECs.

3.6. Effect of blebbistatin on NMMHC IIA/ Wnt5a/β-catenin signaling pathway in LPS-stimulated HUVECs

To further clarify the effect and mechanism of blebbistatin in inhibiting LPS-induced endothelial barrier dysfunction, HUVECs were pretreated with blebbistatin (1 μmol/L) 1 h before LPS (5 μg/mL) exposure and the samples of HUVECs were collected at 6 h after LPS challenge. The western blot results showed that blebbistatin (1 μmol/L) significantly inhibited the increase of NMMHC IIA and Wnt5a expression and the decrease of β-catenin expression in HUVECs of the model group (Fig. 7, A–C). These results suggested that blebbistatin could protect LPS-induced endothelial cell barrier dysfunction by modulating NMMHC IIA/Wnt5a/β-catenin signaling pathway.

3.7. Effect of blebbistatin on LPS-induced dissociation between NMMHC IIA and TLR4 protein in MLECs

To investigate the interaction between NMMHC IIA and TLR4 in endothelial cells, Immunofluorescence co-localization, Co-IP, and PLA techniques were used. In the resting state, both NMMHC IIA (green fluorescence) and TLR4 (red fluorescence) were located in the proximal membrane region and the cytoplasm (orange fluorescence). After LPS

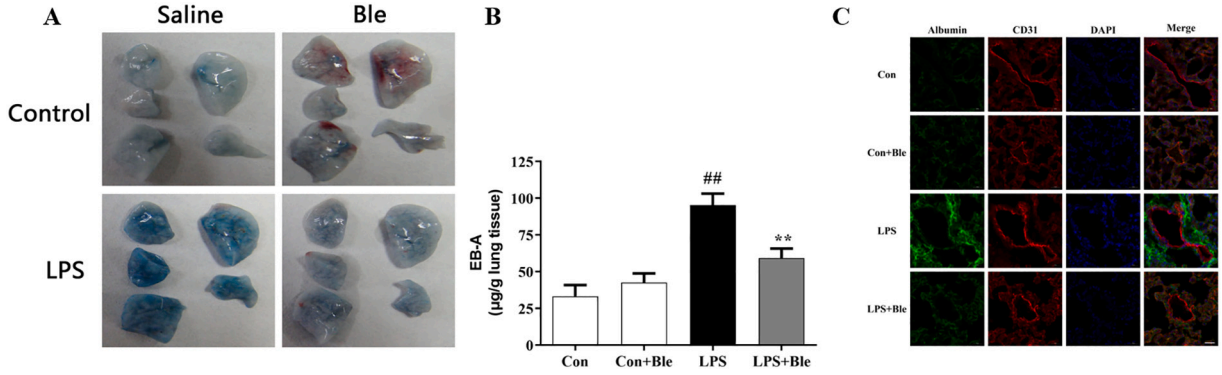

Fig. 2. Blebbistatin alleviated LPS-induced pulmonary vascular hyperpermeability in mice. (A-B) At 4 h After LPS administration, mice were intravenously injected with EBA. After 2 h, the dye was extracted from lung tissues and quantified to determine the effects of blebbistatin on LPS-induced the extravasation of evans blue dye albumin into lung parenchyma. (C) Immunofluorescence for extravascular albumin (green) and CD31 (red) in lung frozen sections, nuclei were stained with DAPI (blue) ($n = 3$). Scale bar: 5 μm. Data are shown as the means ± SD (A-B). $n = 8$. (C). $n = 3$. $^{\#\#}P < 0.01$ vs. the control group; $^{**}P < 0.01$ vs. the LPS group.

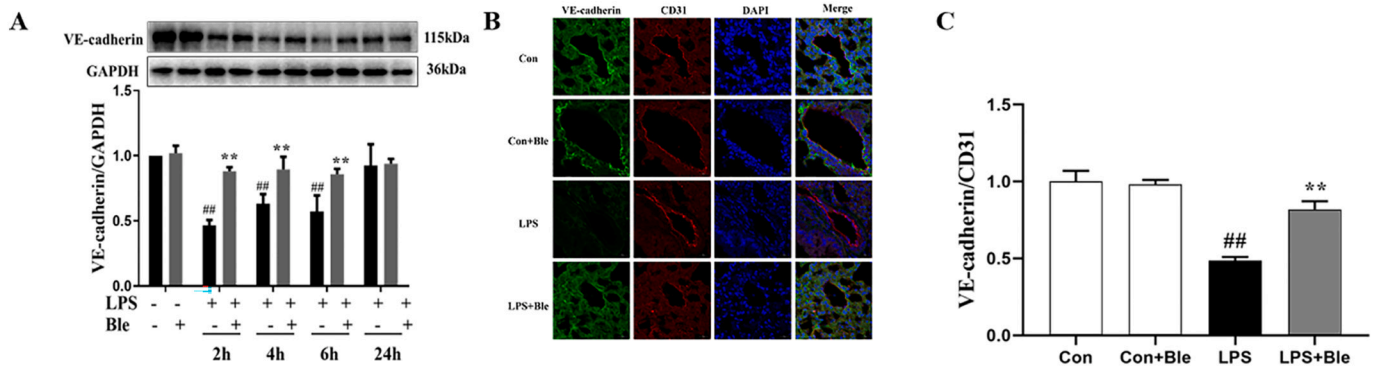

Fig. 3. Blebbistatin inhibited LPS-induced decrease of VE-cadherin expression in lung tissues. Mice were injected intraperitoneally with blebbistatin (5 mg/kg) for 1 h prior to LPS instillation for. 2, 4, 6, 24 h. (A) Effect of blebbistatin on LPS-induced VE-cadherin total protein expression in lung tissues was analyzed by western blotting. (B) Immunofluorescence staining for VE-cadherin (green) and CD31 (red) were performed on frozen lung sections, and the nuclei were stained with DAPI (blue). Scale bar=20 μm. (C) The fluorescence intensity of these proteins in lung endothelium was quantified by Image J (n = 3). Data are shown as the means ± SD (A-C). n = 3. $^{\#\#}P < 0.01$ vs. the control group; $^{**}P < 0.01$ vs. the LPS group.

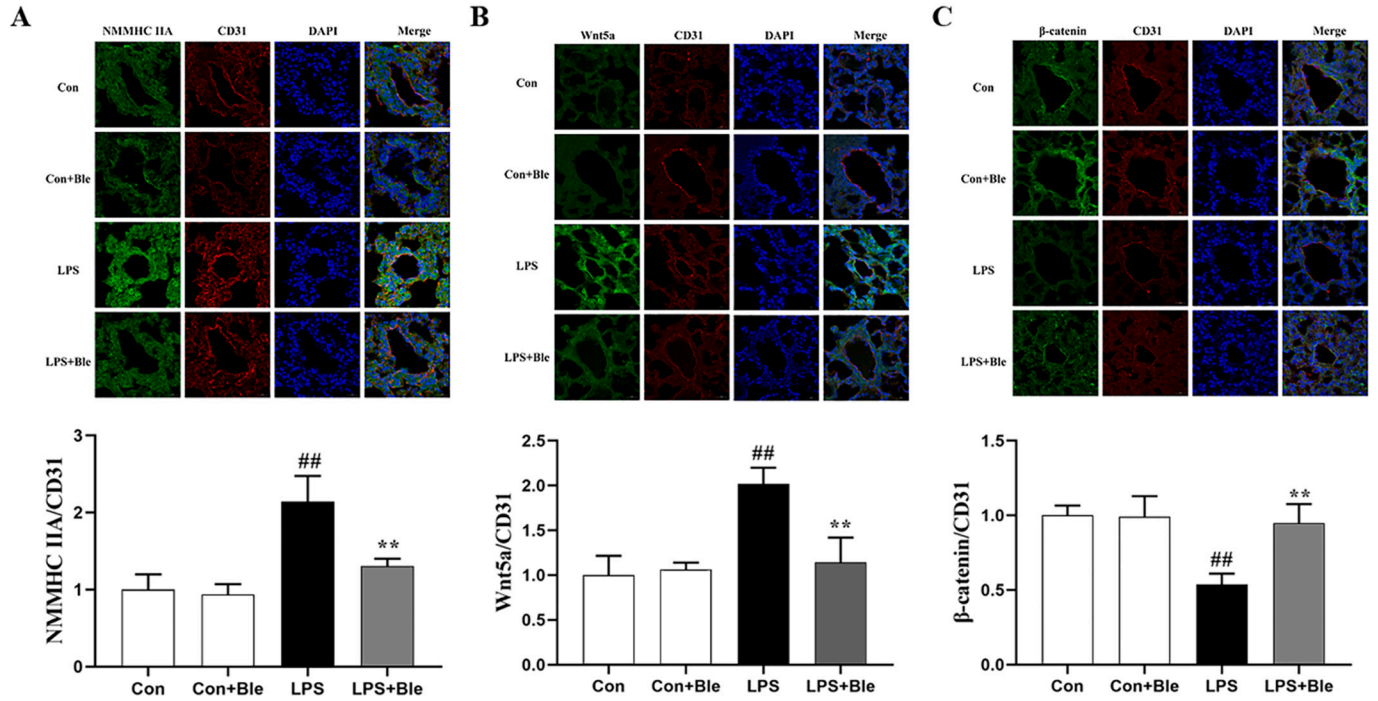

Fig. 4. Blebbistatin inhibited LPS-induced activation of NMMHC IIA/Wnt5a/β-catenin signaling pathway in pulmonary endothelium in mice. Immunofluorescence staining for (A) NMMHC IIA, (B) Wnt5a, (C) β-catenin, (green) and CD31 (red) were performed on frozen lung sections, and the nuclei were stained with DAPI (blue). Scale bar =20 μm. The fluorescence intensity of these proteins in lung endothelium was quantified by Image J ($n = 3$). Data are shown as the means ± SD (A-C). $n = 3$. $^{\#\#}P < 0.01$ vs. the control group; $^{**}P < 0.01$ vs. the LPS group.

(300 ng/mL) stimulation for 1 h, NMMHC IIA was transferred from the proximal membrane region to the center, forming cross-cell stress fibers. However, when blebbistatin (1 μmol/L) was administered, it significantly inhibited the translocation of NMMHC IIA. It promoted the return of NMMHC IIA to the proximal membrane region and cytoplasm, overlapping with the location of TLR4 (Fig. S2 A). Co-IP results showed that NMMHC IIA was associated with TLR4 protein in primary lung endothelial cells in the resting state. After LPS stimulation (300 ng/mL) for 1 h, NMMHC IIA dissociated from TLR4 protein. However, after blebbistatin administration, it significantly inhibited the dissociation of TLR4 and NMMHC IIA proteins in LPS-stimulated primary lung endothelial cells (Fig. S2 B). At the same time, the PLA technique further confirmed the above results. Both the blank and blebbistatin groups showed red bright spot fluorescence (indicating the interaction between two proteins). In contrast, the LPS group showed no or rare red bright spot fluorescence (Fig. S2 C). These results suggested that blebbistatin significantly inhibited the dissociation of TLR4 and NMMHC IIA proteins in LPS-stimulated primary pulmonary endothelial cells.

4. Discussion

The present study used LPS intratracheal installation to establish an ALI mouse model. The role of blebbistatin in the pulmonary endothelial barrier in LPS-induced ALI was studied. Additionally, the function of blebbistatin in LPS-induced endothelial barrier disruption of MLECs and HUVECs was evaluated, and the mechanism of blebbistatin on the endothelial barrier was associated with NMMHC IIA/Wnt5a/β-catenin signaling pathway. Collectively, these data suggested that blebbistatin might have a role in protecting against the pulmonary endothelial barrier in an LPS-induced model in vivo and in vitro.

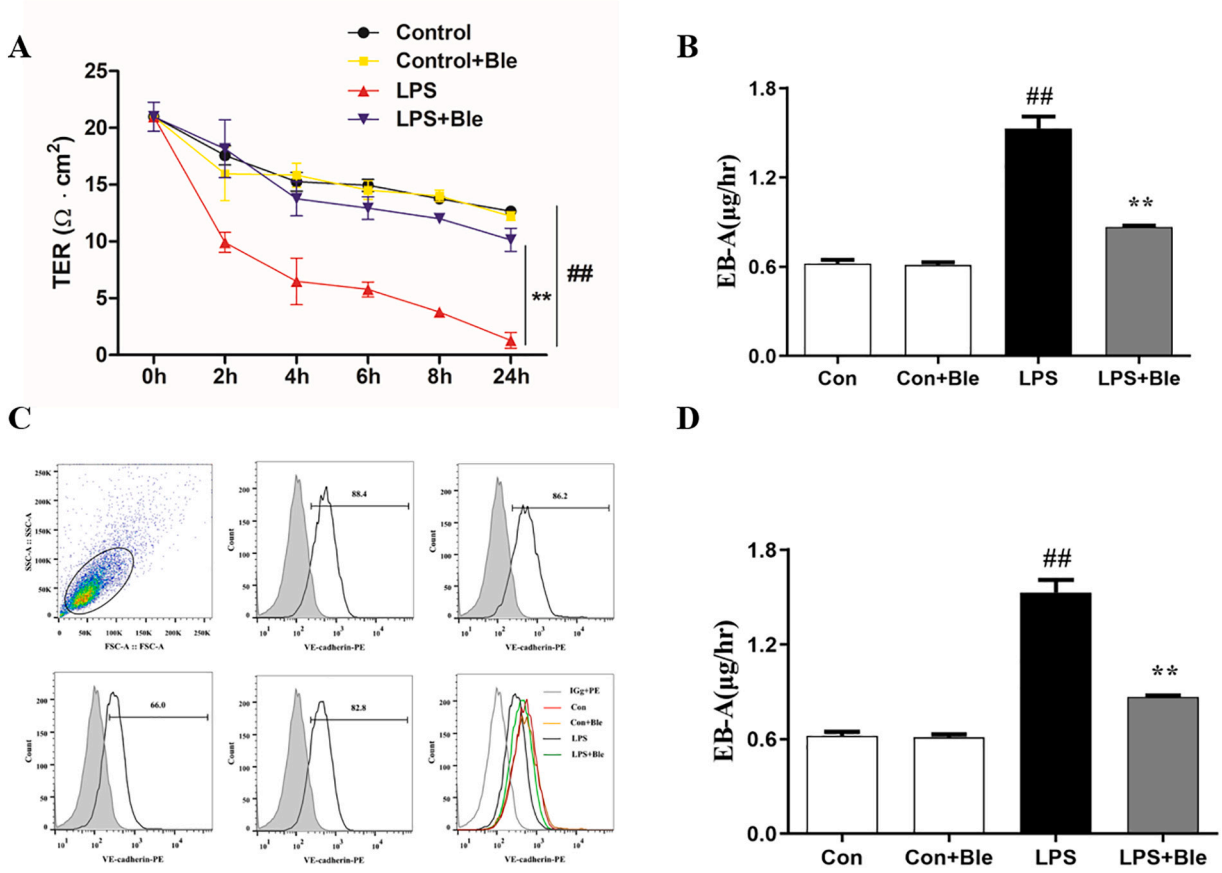

Fig. 5. Blebbistatin inhibited LPS-induced MLECs hyperpermeability. MLECs seeded on gelatincoated transwell inserts for 5–6 days formed a monolayer, which was administrated with blebbistatin (1 μmol/L) for 1 h prior to LPS (300 ng/ml) stimulation for 6 h. (A) The effect of blebbistatin on LPS-induced decrease in MLECs TEER was determined by Millicell-ERS resistance instrument. (B) The effect of blebbistatin on LPS-induced MLECs hyperpermeability was detected by EBA. (C–D) Effect of blebbistatin on LPS-induced decrease of VE-cadherin protein content in MLECs membrane was analyzed by flow cytometry. Data are shown as the means ± SD (A-B). $n = 6$. (C–D). n = 3. $^{\#\#}P < 0.01$ vs. the control group; $^{**}P < 0.01$ vs. the LPS group.

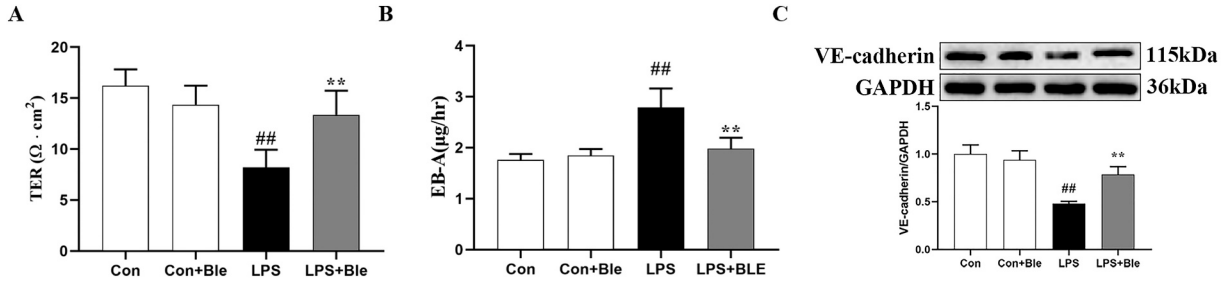

Fig. 6. Blebbistatin inhibited LPS-induced HUVECs hyperpermeability. HUVECs seeded on gelatincoated transwell inserts for 5–6 days formed a monolayer, which was administrated with blebbistatin (1 μmol/L)) for 1 h prior to LPS (5 μg/ml) stimulation for 6 h. (A) The effect of blebbistatin on LPS-induced decrease in HUVECs TEER was determined by Millicell-ERS resistance instrument. (B) The effect of blebbistatin on LPS-induced HUVECs hyperpermeability was detected by Evans blue-labeled albumin. (C) Effect of blebbistatin on LPS-induced decrease of VE-cadherin expression in HUVECs were measured by western blotting. Data are shown as the means ± SD (A-B). n = 6. (C). n = 3. $^{\#\#}P < 0.01$ vs. the control group; $^{**}P < 0.01$ vs. the LPS group.

ALI, and its severe phase ARDS, is a severe inflammatory disease of the lungs with high morbidity and mortality, characterized by respiratory distress, progressive hypoxemia, and pulmonary edema. ALI can be caused by bacteria, viruses, pneumonia, and other pathogenic factors. Currently, the primary treatment is mechanical ventilation and oxygenation, and there is no effective treatment for the basic pathophysiology of ALI/ARDS. ALI can be divided into three stages: exudate stage, hyperplasia stage, and fibrosis stage. In the early exudate stage in ALI, the stimulation of pathogenic factors promotes the transformation of endothelial cells from an anti-inflammatory to a pro-inflammatory phenotype, thus inducing neutrophils and inflammatory cell aggregation, inducing the inflammatory cascade reaction, destroying the endothelial barrier function, eventually leading to the pulmonary edema, respiratory distress, and hypoxemia, and increases mortality in ALI patients (Bellani et al., 2016; Matthay et al., 2019; Thompson et al., 2017). Therefore, the destruction of the pulmonary endothelial barrier is the most fundamental pathological feature of ALI (Müller Redetzky et al., 2014). Protecting pulmonary endothelial barrier function may be an effective therapeutic strategy for preventing and treating ALI.

AJs are particularly important in the pulmonary vascular endothelial barrier, and their dynamic and rapid synthesis, assembly, and degradation maintain the semi-permeability of the endothelial barrier

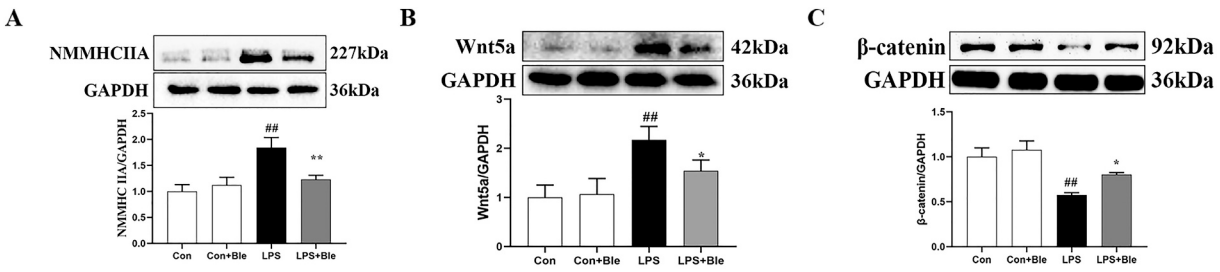

Fig. 7. Blebbistatin inhibited LPS-induced activation of NMMHC IIA/Wnt5a/β-catenin signal pathway in HUVECs. HUVECs were administrated with blebbistatin (1 μmol/L) for 1 h prior to LPS (5 μg/ml) stimulation for 6 h. Effect of blebbistatin on LPS-induced (A) NMMHC IIA, (B) Wnt5a, and (C) β-catenin expression in HUVECs were measured by western blotting. Data are shown as the means ± SD (A-C). n = 3. $^{\#\#} < 0.01$ vs. the control group; $^{*}P < 0.05$, $^{**}P < 0.01$ vs. the LPS group.

(Bhattacharya and Matthay, 2013). Therein, VE-cadherin is an integral part of AJs and maintains the stability of the pulmonary endothelial barrier by binding to the extracellular structure of adjacent endothelial cells (Harris and Nelson, 2010; Gavard, 2014). Therefore, the change of VE-cadherin expression can reflect the status of pulmonary endothelial barrier function. Our results suggested that blebbistatin protected against LPS-induced destruction of the pulmonary endothelial barrier in vivo and in vitro. Blebbistatin could improve the destruction of LPS-induced lung tissue morphology and the leakage of EBA, reduce the infiltration of neutrophils and protein, and improve the expression of VE-cadherin in lung tissues induced by LPS at different times. Consistent with our results, previous studies have shown that NMMHC IIA knockdown can maintain endothelial barrier function, playing a role in the prevention and treatment of ischemic stroke and ALI (Gong et al., 2021; Wu et al., 2021). In addition, our results also confirm the idea mentioned in the previous article that blebbistatin, as inhibitors and tool agents of NMMHC II, are involved in functional studies of NMMHC IIA in a variety of diseases and physiological conditions (Wang et al., 2017).

In addition, previous pathological studies have proved that NMMHC IIA binds to TLR4 in the endothelium under normal physiological conditions to inhibit the transmission of the TLR4 inflammatory pathway. When LPS stimulates endothelial cells, NMMHC IIA dissociates from TLR4 and activates downstream Src kinase, which further promotes the depolymerization of the adhesion of VE-cadherin and its intracellular anchor protein P120-catenin. Finally, VE-cadherin is endocytosed to intracellular degradation. The content of VE-cadherin on the cell membrane is reduced, destroying the endothelial barrier. Meanwhile, knockdown of NMMHC IIA can improve endothelial barrier dysfunction by reversing LPS-induced dissociation of NMMHC IIA from TLR4 and inhibiting downstream pathways. In addition, these drugs targeting NMMHC IIA regulate NMMHC IIA related signaling pathways by acting on the part of NMMHC IIA. Among them, NMMHC IIA binding functional regions mainly include the N-terminal containing actin-binding site, the Head functional region containing ATPase activity site, and the C-terminal tail functional region involved in the formation of filaments. For example, ruscogenin regulates the interaction between NMMHC IIA and TLR4 by acting on NMMHC IIA N-terminal and Head domain functional regions, inhibiting the TLR4 signaling pathway, and thus plays a protective role in LPS-induced endothelial barrier dysfunction (Wu et al., 2021). Our results show that blebbistatin could regulate the interaction between NMMHC IIA and TLR4 by acting on the sites of ATPase of NMMHC IIA, and inhibit the LPS-induced dissociation of NMMHC IIA and TLR4, thus inhibiting the activation of TLR4 signaling pathway and ultimately protecting LPS-induced endothelial barrier dysfunction. The above results suggest that different drugs that bind to various sites of the same protein may have the same effect.

In the study of the protective mechanism of blebbistatin on pulmonary endothelial barrier function , our results reflected that after LPS stimulation for 6 h, the expression of NMMHC IIA and Wnt5A was increased in lung tissue and HUVECs. In contrast, the expression of β-catenin was significantly decreased. At the same time, blebbistatin inhibited LPS-induced related proteins expression changes. These results demonstrated that blebbistatin protected pulmonary endothelial barrier function by regulating NMMHC IIA/Wnt5a/β-catenin signaling pathway.

The relationship between Wnt/β-catenin and ALI has been studied in the early stage, among which Wnt5a and Wnt3a play different roles. Therein, β-catenin, as a skeletal protein, plays a role in the stability of VE-cadherin in endothelial cells, and studies have shown that LPS-induced disruption of pulmonary endothelial barrier leads to β-catenin degradation (Rho et al., 2017; Tharakan et al., 2012; Weng et al., 2019; Zhu et al., 2019). Meanwhile, Wnt3a/β-catenin as a classical pathway is involved in maintaining endothelial barrier function, and Wnt3a activation improves ALI(Hii et al., 2015). However, studies have shown that the expression of Wnt5a is elevated in the ALI model, and inhibiting Wnt5a attenuates the progress of ALI (Villar et al., 2014). Interestingly, there is a mismatch between the conclusion in some literature with our experimental results. Studies have shown that in various ALI models, including the mechanical ventilation-induced ALI model, the expression of β-catenin in the model group is significantly increased, promoting tissue proliferation and fibrosis, and inhibiting β-catenin could inhibit ALI (Villar et al., 2014). We speculated that there might be two reasons. First, these studies focus more on the middle and late stages of ALI, hyperplasia, and fibrosis than the pathological process of early leakage in ALI. Secondly, these studies mainly focused on epithelial cells and lacked the detection of endothelial barrier function.

In conclusion, our results demonstrated that blebbistatin, as a non-specific inhibitor of NMMHC IIA, could also inhibit LPS-induced damage of pulmonary endothelial barrier function and thus play a protective role against ALI. Meanwhile, blebbistatin was protective of endothelial barrier in vivo and in vitro through NMMHC IIA/Wnt5a/β-catenin signaling pathways. This study demonstrated the effectiveness of protective endothelial barrier function in the prevention and treatment of ALI disease, providing a new therapeutic strategy for the prevention and treatment of ALI and increasing the related downstream mechanism of the protective endothelial barrier function of NMMHC IIA.

Although our study preliminarily demonstrated that blebbistatin could protect the endothelial barrier function through NMMHC IIA/Wnt5a/β-catenin signaling pathways, thus playing a role in preventing ALI. However, the phototoxicity and solubility of blebbistatin have seriously affected the development of blebbistatin as a drug. Meanwhile, blebbistatin, as a non-specific inhibitor of NMMHC IIA, can't fully prove the relationship between NMMHC IIA and the Wnt5a/β-catenin signaling pathway, which may need to be discussed in a new paper.

In summary, we demonstrated that the NMMHC IIA inhibitor blebbistatin could inhibit LPS-induced endothelial barrier disruption in vivo and in vitro, at least in part, via NMMHC IIA/Wnt5a/β-catenin signaling pathway. These findings identified that blebbistatin might have potential clinical applications for preventing and treating ALI.

Ethics approval and consent to participate

All the experimental protocols in this study were approved by the Institutional Animal Care and Use Committee of China Pharmaceutical University. All authors consent to participate in this research.

Consent for publication

All authors consent to publish this article.

Availability of data and materials

The data used to support the findings of this study are available from the corresponding author upon request.

Funding

This work was supported by the National Natural Science Foundation of China (No. 81773971).

Authors' contribution

JZZ, YYZ, and JPK designed the project; JZZ, ZQP, JHZ, LZ, and JHT performed the experiments; JZZ and ZQP contributed to analyzing the data; JZZ conducted the literature research; JZZ organized the results and drafted the original manuscript; JZZ, ZQP, YYZ, and JPK reviewed and modified the manuscript; SSG, FL, BYY, YYZ, and JPK contributed to the funding acquisition.

CRediT authorship contribution statement

Jiazhi Zhang: Conceptualization, Methodology, Software, Investigation, Formal analysis, Writing – original draft, Writing – review & editing. **Ziqian Pan:** Investigation, Data curation, Writing – original draft. **Jianhao Zhou:** Visualization, Investigation. **Ling Zhang:** Investigation. **Jiahui Tang:** Investigation. **Shuaishuai Gong:** Visualization, Funding acquisition. **Fang Li:** Funding acquisition. **Boyang Yu:** Funding acquisition. **Yuanyuan Zhang:** Conceptualization, Funding acquisition, Supervision, Writing – review & editing. **Junping Kou:** Conceptualization, Funding acquisition, Resources, Supervision, Writing – review & editing.

Declaration of Competing Interest

The authors declare that there are no conflicts of interest.

Appendix A. Supplementary data

Supplementary data to this article can be found online at https://doi.org/10.1016/j.taap.2022.116132.

References

Bellani, G., Laffey, J.G., Pham, T., Fan, E., Brochard, L., Esteban, A., 2016. Epidemiology, patterns of care, and mortality for patients with acute respiratory distress syndrome in intensive care units in 50 countries. JAMA. 315, 788–800.
Bhattacharya, J., Matthay, M.A., 2013. Regulation and repair of the alveolar-capillary barrier in acute lung injury. Annu. Rev. Physiol. 75, 593–615.
Bolte, S., Cordelières, F.P., 2006. A guided tour into subcellular colocalization analysis in light microscopy. J. Microsc. 224, 213–232.
Chen, L., Li, W., Qi, D., Lu, L., Zhang, Z., Wang, D., 2018. Honokiol protects pulmonary microvascular endothelial barrier against lipopolysaccharide-induced ARDS partially via the Sirt3/AMPK signaling axis. Life Sci. 210, 86–95.
Conti, M.A., Even-Ram, S., Liu, C., Yamada, K.M., Adelstein, R.S., 2004. Defects in cell adhesion and vBiol. Chem. 279, 41263–41266.
Dong, W., He, B., Qian, H., Liu, Q., Wang, D., Li, J., 2018. RAB26-dependent autophagy protects adherens junctional integrity in acute lung injury. Autophagy. 14, 1677–1692.
Fazal, F., Bijli, K.M., Murrill, M., Leonard, A., Minhajuddin, M., Anwar, K.N., 2013. Critical role of non-muscle myosin light chain kinase in thrombin-induced endothelial cell inflammation and lung PMN infiltration. PLoS One 8, e59965.
Gavard, J., 2014. Endothelial permeability and VE-cadherin: a wacky comradeship. Cell Adhes. Migr. 8, 158–164.
Gong, P., Angelini, D.J., Yang, S., Xia, G., Cross, A.S., Mann, D., 2008. TLR4 signaling is coupled to SRC family kinase activation, tyrosine phosphorylation of zonula adherens proteins, and opening of the paracellular pathway in human lung microvascular endothelia. J. Biol. Chem. 283, 13437–13449.
Gong, H., Rehman, J., Tang, H., Wary, K., Mittal, M., Chaturvedi, P., 2015. HIF2α signaling inhibits adherens junctional disruption in acute lung injury. J. Clin. Invest. 125, 652–664.
Gong, S., Cao, G., Li, F., Chen, Z., Pan, X., Ma, H., 2021. Endothelial conditional knockdown of NMMHC IIA (nonmuscle myosin heavy chain IIA) attenuates blood-brain barrier damage during ischemia-reperfusion injury. Stroke. 52, 1053–1064.
Gorudko, I.V., Grigorieva, D.V., Sokolov, A.V., Shamova, E.V., Kostevich, V.A., Kudryavtsev, I.V., 2018. Neutrophil activation in response to monomeric myeloperoxidase. Biochem. Cell Biol. 96, 592–601.
Harris, E.S., Nelson, W.J., 2010. VE-cadherin: at the front, center, and sides of endothelial cell organization and function. Curr. Opin. Cell Biol. 22, 651–658.
Hii, H.P., Liao, M.H., Chen, S.J., Wu, C.C., Shih, C.C., 2015. Distinct patterns of Wnt3a and Wnt5a signaling pathway in the lung from rats with endotoxic shock. PLoS One 10, e0134492.
Kitching, A.R., Anders, H.J., Basu, N., Brouwer, E., Gordon, J., Jayne, D.R., 2020. ANCA-associated vasculitis. Nature reviews. Dis. Prim. 6, 71.
Lim, Y.C., Garcia-Cardena, G., Allport, J.R., Zervoglos, M., Connolly, A.J., Gimbrone Jr., M.A., 2003. Heterogeneity of endothelial cells from different organ sites in T-cell subset recruitment. Am. J. Pathol. 162, 1591–1601.
Liu, A., Gong, P., Hyun, S.W., Wang, K.Z., Cates, E.A., Perkins, D., 2012. TRAF6 protein couples toll-like receptor 4 signaling to Src family kinase activation and opening of paracellular pathway in human lung microvascular endothelia. J. Biol. Chem. 287, 16132–16145.
Matthay, M.A., Zemans, R.L., Zimmerman, G.A., Arabi, Y.M., Beitler, J.R., Mercat, A., 2019. Acute respiratory distress syndrome. Nature reviews. Disease primers. 5, 18.
Millar, F.R., Summers, C., Griffiths, M.J., Toshner, M.R., Proudfoot, A.G., 2016. The pulmonary endothelium in acute respiratory distress syndrome: insights and therapeutic opportunities. Thorax. 71, 462–473.
Müller Redetzky, H.C., Suttorp, N., Witzenrath, M., 2014. Dynamics of pulmonary endothelial barrier function in acute inflammation: mechanisms and therapeutic perspectives. Cell Tissue Res. 355, 657–673.
Naydenov, N.G., Feygin, A., Wang, D., Kuemmerle, J.F., Harris, G., Conti, M.A., 2016. Nonmuscle myosin IIA regulates intestinal epithelial barrier in vivo and plays a protective role during experimental colitis. Sci. Rep. 6, 24161.
Pierre, S., Scholich, K., 2010. Toponomics: studying protein-protein interactions and protein networks in intact tissue. Mol. BioSyst. 6, 641–647.
Rho, S.S., Ando, K., Fukuhara, S., 2017. Dynamic regulation of vascular permeability by vascular endothelial cadherin-mediated endothelial cell-cell junctions. J. Nippon Med. School = Nippon Ika Daigaku zasshi. 84, 148–159.
Sun, X., Sun, B.L., Sammani, S., Bermudez, T., Dudek, S.M., Camp, S.M., 2021. Genetic and epigenetic regulation of the non-muscle myosin light chain kinase isoform by lung inflammatory factors and mechanical stress. Clin. Sci. (Lond.). 135, 963–977.
Tharakan, B., Hellman, J., Sawant, D.A., Tinsley, J.H., Parrish, A.R., Hunter, F.A., 2012. β-Catenin dynamics in the regulation of microvascular endothelial cell hyperpermeability. Shock. 37, 306–311.
Thompson, B.T., Chambers, R.C., Liu, K.D., 2017. Acute respiratory distress syndrome. N. Engl. J. Med. 377, 562–572.
Villar, J., Cabrera-Benítez, N.E., Ramos-Nuez, A., Flores, C., García-Hernández, S., Valladares, F., 2014. Early activation of pro-fibrotic WNT5A in sepsis-induced acute lung injury. Crit. Care 18, 568.
Villar, J., Blanco, J., Kacmarek, R.M., 2016. Current incidence and outcome of the acute respiratory distress syndrome. Curr. Opin. Crit. Care 22, 1–6.
Wang, Y., Xu, Y., Liu, Q., Zhang, Y., Gao, Z., Yin, M., 2017. Myosin IIA-related actomyosin contractility mediates oxidative stress-induced neuronal apoptosis. Front. Mol. Neurosci. 10, 75.
Wang, G., Wang, T., Hu, Y., Wang, J., Wang, Y., Zhang, Y., 2020a. NMMHC IIA triggers neuronal autophagic cell death by promoting F-actin-dependent ATG9A trafficking in cerebral ischemia/reperfusion. Cell Death Dis. 11, 428.
Wang, G.Y., Wang, T.Z., Zhang, Y.Y., Li, F., Yu, B.Y., Kou, J.P., 2020b. NMMHC IIA inhibition ameliorates cerebral ischemic/reperfusion-induced neuronal apoptosis through Caspase-3/ROCK1/MLC pathway. Drug Des. Devel. Ther. 14, 13–25.
Weng, J., Yu, L., Chen, Z., Su, H., Yu, S., Zhang, Y., 2019. β-Catenin phosphorylation at Y654 and Y142 is crucial for high mobility group box-1 protein-induced pulmonary vascular hyperpermeability. J. Mol. Cell. Cardiol. 127, 174–184.
Wu, G., Chang, F., Fang, H., Zheng, X., Zhuang, M., Liu, X., 2021. Non-muscle myosin II knockdown improves survival and therapeutic effects of implanted bone marrow-derived mesenchymal stem cells in lipopolysaccharide-induced acute lung injury. Ann. Transl. Med 9, 262.
Wu, Y., Yu, X., Wang, Y., Huang, Y., Tang, J., Gong, S., 2021. Ruscogenin alleviates LPS-triggered pulmonary endothelial barrier dysfunction through targeting NMMHC IIA to modulate TLR4 signaling. Acta Pharm. Sin. B 111–121.

Xiao, K., Garner, J., Buckley, K.M., Vincent, P.A., Chiasson, C.M., Dejana, E., 2005. p120-catenin regulates clathrin-dependent endocytosis of VE-cadherin. Mol. Biol. Cell 16, 5141–5151.

Yu, J., Ma, Z., Shetty, S., Ma, M., Fu, J., 2016. Selective HDAC6 inhibition prevents TNF-α-induced lung endothelial cell barrier disruption and endotoxin-induced pulmonary edema. Am. J. Phys. Lung Cell. Mol. Phys. 311, L39–L47.

Zhai, K.F., Zheng, J.R., Tang, Y.M., Li, F., Lv, Y.N., Zhang, Y.Y., 2017. The saponin D39 blocks dissociation of non-muscular myosin heavy chain IIA from TNF receptor 2, suppressing tissue factor expression and venous thrombosis. Br. J. Pharmacol. 174, 2818–2831.

Zhu, N., Zhang, G.X., Yi, B., Guo, Z.F., Jang, S., Yin, Y., 2019. Nur77 limits endothelial barrier disruption to LPS in the mouse lung. Am. J. Phys. Lung Cell. Mol. Phys. 317, L615–l624.